1′,5′-Anhydrohexitol Oligonucleotides: Synthesis, Base Pairing and Recognition by Regular Oligodeoxyribonucleotides and Oligoribonucleotides

Chris Hendrix, Helmut Rosemeyer, Ilse Verheggen, Frank Seela, Arthur Van Aerschot and Piet Herdewijn*

Abstract: Oligonucleotides constructed of 1′,5′-anhydrohexitol nucleoside building blocks (hexitol nucleic acids, HNA) are completely stable towards 3′-exonuclease and form very stable self-complementary duplexes as well as sequence-selective stable duplexes with the natural DNA and RNA. Triple-helix formation has also been observed. These hybridisation characteristics are highly dependent on the base sequence and the experimental conditions. When using a phosphate buffer containing 0.1 M NaCl, a homopurine HNA dodecamer gives a ΔT_m of +1.3 °C/base pair with DNA as complement and a ΔT_m of +3.0 °C/base pair with RNA as complement. These oligomers may therefore be of considerable interest as antisense constructs.

Keywords
antisense systems · DNA recognition · nucleic acids · oligonucleotides · RNA

Introduction

New oligonucleotide constructs designed to hybridise strongly with complementary DNA or RNA can be synthesised from modified bases or an altered sugar–phosphate backbone.[1]

The incorporation of modified bases into oligonucleotides often leads to less stable duplexes, but some exceptions have been found recently in the purine and in the pyrimidine series: 1) Oligonucleotides having 7-halogeno-7-deaza-2′-deoxyadenosine residues instead of 2′-deoxyadenosine exhibit significantly increased duplex stability.[2] 2) Similar results have been obtained for oligonucleotides in which 2′-deoxyguanosine is replaced by 8-aza-2′-deoxyguanosine.[3] 3) Alkynyl derivatives of regular and modified bases[4] and tricyclic 2′-deoxycytidine analogues[5] also show these favourable properties.

In the case of the backbone-modified compounds, oligo(2′-deoxyxylonucleotides), which represent an alternative DNA with a configurationally altered sugar–phosphate backbone, have been synthesised. They show a sequence-dependent duplex stabilisation relative to the corresponding oligo(2′-deoxyribonucleotides).[6] However, the most important backbone-modified compounds incorporate altered internucleotide linkages, leading to stabilised duplexes, such as the thioformacetal group 3′-S-CH_2-O-CH_2-4′,[7] the methylene(methylimino) backbone 3′-CH_2-N(CH_3)-O-CH_2-4′,[8] the methylene amide spacer 3′-CH_2-CO-NH-CH_2-4′[9] and the N 3′ → P 5′ phosphoramidates.[10] Similar results have been found for other sugar modifications (e.g. 2′-*O*-methylribonucleosides,[11] carbocyclic nucleosides,[12] α-nucleosides[13]).

Plenty of information is available about the duplex stability of oligonucleotides with single phosphate replacements or backbone structures with alternating phosphate– and nonphosphate–internucleotide linkages.[14] However, completely backbone-modified oligonucleotides have rarely been synthesised. This is due to the lack of methods available to oligomerize such structures. Two important examples of nonphosphate oligonucleotides with a completely modified backbone are the morpholinocarbamate-linked oligonucleotides[15] and the polyamide-linked acyclic nucleic acids (peptide nucleic acids or PNAs).[16] Structural alterations of this type that have been integrated into oligonucleotides have been reviewed recently.[17]

In principle, an increase in the T_m values as a result of the incorporation of a modified nucleoside will not lead, per se, to a promising antisense construct. Other factors such as RNase H activation, selectivity of hybridisation, cellular uptake, nuclease stability and metabolic behaviour are at least as important as the hybridisation strength. However, it seems obvious that the higher the stability of the duplex formed between natural RNA and the antisense oligonucleotide, the greater the possibility of physical blockage of the targeted mRNA being sufficient to inhibit the translation process.

[*] Prof. Dr. P. Herdewijn, Dr. C. Hendrix, Dr. I. Verheggen, Dr. A. Van Aerschot
Laboratory of Medicinal Chemistry, Rega Institute for Medical Research
Katholieke Universiteit Leuven, Minderbroedersstraat 10
B-3000 Leuven
(Belgium)
Fax: Int. code +(16)337387
e-mail: piet.herdewijn@rega.kuleuven.ac.be
Dr. H. Rosemeyer, Prof. Dr. F. Seela
Laboratorium für Organische & Bioorganische Chemie
Institut für Chemie, Universität Osnabrück
Barbarastrasse 7, 49069 Osnabrück (Germany)

0947-6539/97/0301-0110 $ 15.00+.25/0

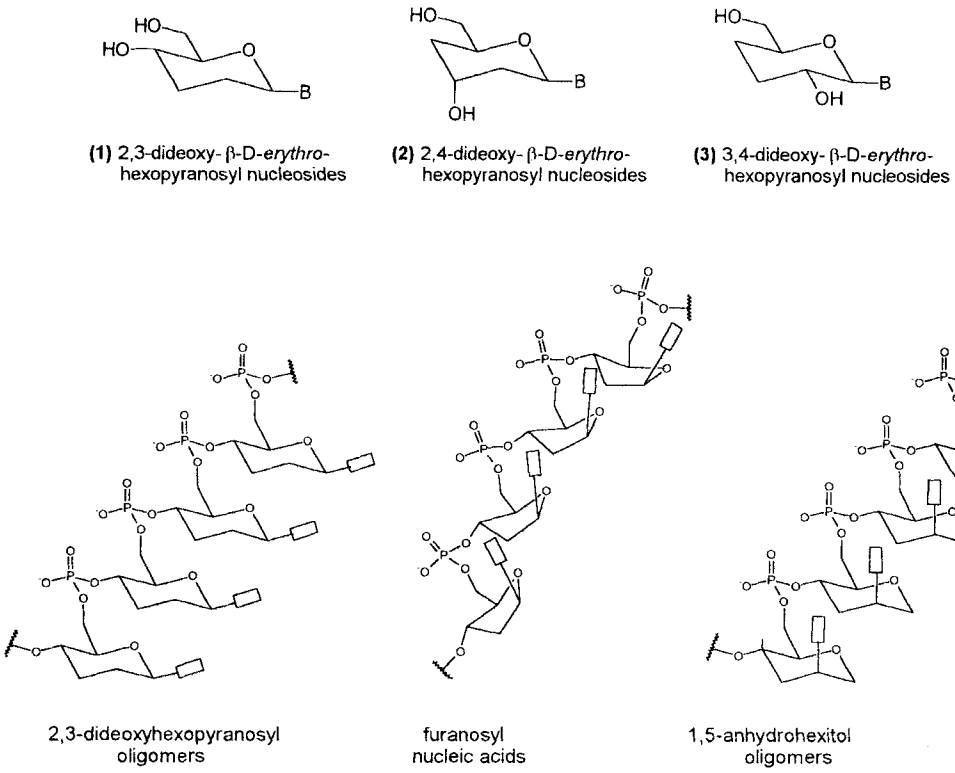

Fig. 1. Structural formulae of some pyranose nucleosides incorporated in oligonucleotides and of pyranosyl, furanosyl and hexitol nucleic acids.

A detailed study of oligonucleotides built up from monomeric pyranose nucleosides has been undertaken by the group of A. Eschenmoser[18–20] and by ourselves.[21–23] While the former laboratory is investigating Nature's selection of furanoses as sugar building blocks for nucleic acids, we have been looking at the problem from the point of view of medicinal chemistry. This means that we have investigated which pyranose-like oligonucleotide would be able to form stable duplexes with natural furanose DNA. Theoretically, a pyranose oligonucleotide has a free energy advantage over a furanose oligomer, because there are less entropy changes during duplex formation.[18, 24] However, the pyranose-like oligonucleotides studied thus far were not able or were not sufficiently able to bind to complementary strands of natural furanose DNA.[18–22] The pyranose-like oligonucleotides that we have studied have been based on nucleosides **1**, **2** or **3** (Figure 1). Studies on pyranose DNA[18] revealed that the structure of oligomers composed of **1** is almost linear; this was attributed to the size and rigidity of the pyranose moiety. It has been shown that the base of the 1′,5′-anhydrohexitol nucleosides adopts an axial configuration that is very similar to natural DNA or RNA, but different to oligonucleotides composed of **1**.[25] Therefore, we assume that the idealised conformation of a 1′,5′-anhydrohexitol oligonucleotide should be linear in analogy with homo-DNA (Figure 1), in which the bases adopt an equatorial conformation.[19] Likewise, the structures of 1′,5′-anhydrohexitol oligonucleotides and natural DNA show the same number of bonds between the repeating units. In the case of the 1′,5′-anhydrohexitol oligonucleotides, however, the two-atom linker between the base moiety and the backbone structure mimics the front part of the furanose ring (Figure 1). The phosphate internucleotide linkage was selected because it should be flexible—it was previously demonstrated that internucleotide linkages that are conformationally too rigid give a drop in duplex stability.[26] The assumed linear conformation with the bases in axial position and the flexibility of the phosphate junction, which allows conformations that are different from the idealised linear one to be adopted, are features promising stable duplexes of HNA and DNA or RNA.

Results and Discussion

Oligonucleotide Synthesis: The syntheses of A*, T* and G*,

1,5-anhydro-2-(adenin-9-yl)-2,3-dideoxy-D-*arabino*-hexitol A*

1,5-anhydro-2,3-dideoxy-2-(thymin-1-yl)-D-*arabino*-hexitol T*

1,5-anhydro-2,3-dideoxy-2-(guanin-9-yl)-D-*arabino*-hexitol G*

which were used to prepare the nucleotide building blocks **4a–c**, have been described previously (Figure 2).[27] The adenine nucleobase of the 4,6-benzylidene-protected nucleoside analogue (Figure 3) was protected at the amino group with a benzoyl moiety, and the guanine base was protected with an isobutyryl group.[27] The benzylidene moiety of compounds **5b,c** was removed with 80% acetic acid yielding **6b,c**. The primary hydroxyl function of the 1′,5′-anhydrohexitol nucleosides **6a,b,c** was protected with a 4,4′-dimethoxytrityl group to afford **7a,b,c**. Conversion to their phosphoramidites **4a,b,c** afforded building blocks suitable for incorporation into an oligonucleotide using standard methods for DNA synthesis on a solid support.[29] Supports with the 1′,5′-anhydrohexitol nucleoside analogues were prepared by succinylation of **7a,b** giving **8a,b**, which were coupled to the amino function of long chain alkylamino controlled pore glass (CPG).[30]

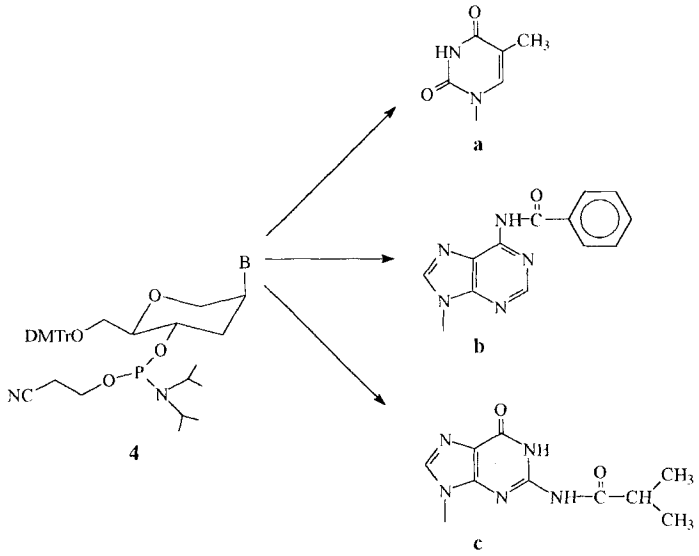

Fig. 2. Phosphoramidite building blocks used for the synthesis of the 1′,5′-anhydrohexitol oligonucleotides.

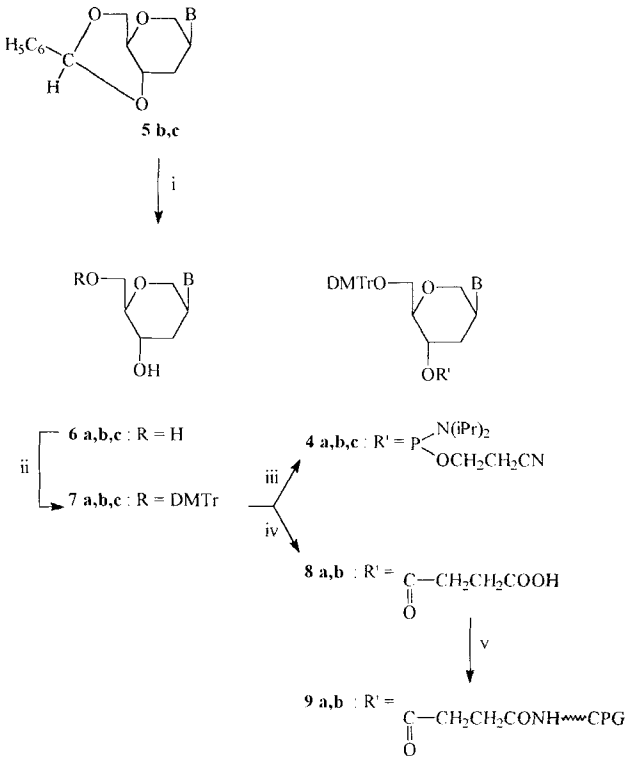

Fig. 3. Synthesis of the 1′,5′-anhydrohexitol nucleoside building blocks for DNA synthesis [**a**: B = thymin-1-yl, **b**: B = N^6-benzoyladenin-9-yl, **c**: B = N^2-isobutyrylguanin-9-yl]. Yields: see Experimental Section. i) 80% HOAc; ii) dimethoxytrityl chloride, pyridine; *iii*) *N,N*-di-isopropylethylamine, 2-cyano-*N,N*-di-isopropylchlorophosphoramidite, CH_2Cl_2; iv) DMAP, succinic anhydride, pyridine; v) preactivated LCAA–CPG, DMAP, Et_3N, 1-(3-diethylaminopropyl)-3-ethylcarbodiimide·HCl, pyridine.

Hybridisation Properties of the 1′,5′-Anhydrohexitol Oligonucleotides: A summary of the synthesised oligonucleotides together with their T_m values is given in Table 1 and Table 2. The oligonucleotides that showed cooperative melting could be evaluated according to a bimolecular all-or-none mechanism.[31, 32] Fitting of a theoretical melting curve to the data resulted in the T_m values as indicated in Table 1.

Table 1. Melting points (°C) observed at 260 nm for oligonucleotides with a single anhydrohexitol nucleoside (A*, T*) incorporated (measured at 4 μM in 0.1 M NaCl, 20 mM KH_2PO_4, pH 7.5, 0.1 mM EDTA).

$(dT)_6\mathbf{X}(dT)_6$
$(dA)_6\mathbf{Y}(dA)_6$

Y	**X**:	G	C	A	T
A		20.0	17.9	18.5	34.0
A*		20.2	17.1	17.7	32.1
X	**Y**:	G	C	T	A
T		21.0	20.7	21.3	34.0
T*		15.1	15.2	18.3	28.7

From Table 1 it is clear that incorporation of A* into an oligodeoxyadenylate gives nearly identical T_m values as the insertion of a natural 2′-deoxyadenosine (A). It should also be mentioned that one mismatch in an oligodeoxyadenylate–oligothymidylate duplex has a large effect on duplex stability. In contrast, replacement of thymidine (T) by T* in an oligothymidylate gives a substantial decrease in melting temperature. Contrary to previous observations that a dA#·dG [dA#: 9-(2,4-dideoxy-β-D-*erythro*-hexopyranosyl)adenine] "base pair" mismatch is more stable than the dA#·T [dA#: 9-(2,4-dideoxy-β-D-*erythro*-hexopyranosyl)adenine] base pair,[23] there is no alteration in base pairing stability of the 1′,5′-anhydrohexitol nucleosides in a oligodeoxyadenylate–oligothymidylate duplex.

The information that can be extracted from Table 2 is of more interest. It summarises the stability of complexes formed between completely modified oligonucleotides and natural DNA,

Table 2. Melting points (°C) observed at 260 nm after mixing equimolar amounts of oligonucleotides containing only anhydrohexitol nucleosides (A*,T*) measured in the following buffers: A: 1 M NaCl, 100 mM $MgCl_2$, 60 mM Na cacodylate, pH 7.0; B: 0.1 M NaCl, 10 mM $MgCl_2$, 10 mM Na cacodylate, pH 7.0; C: 0.1 M NaCl, 0.1 mM EDTA, 0.02 M KH_2PO_4, pH 7.5; D: 10 mM $MgCl_2$ added to buffer C. Concentration of oligonucleotides: 4 μM of each single-strand oligomer (except for oligo-$(T^*)_{13}$·oligo$(A^*)_{13}$, 1.2 μM each).

	T_m(A)	T_m(B)	T_m(C)	T_m(D)
oligo$(T)_{13}$·oligo$(dA)_{13}$	50	42	34	41
oligo$(T)_{13}$·oligo$(A^*)_{13}$	30	15	21	17
oligo$(T^*)_{13}$·oligo$(dA)_{13}$	45 [a]	60	45 [b]	39
			58	56
				71
oligo$(T^*)_{13}$·oligo$(A^*)_{13}$	81	82	76	80
oligo$(T^*)_{13}$·oligo$(T^*)_{13}$	45	–	–	ND [c]
oligo$(A^*)_{13}$·oligo$(A^*)_{13}$	–	–	–	ND

[a] The T_m measured is the T_m of $(T^*)_{13}$·$(T^*)_{13}$. [b] The T_m measured at 284 nm shows a transition at 45 °C, possibly indicating triple-helix formation. [c] ND: not determined.

determined in a series of buffers. When equimolar amounts of oligo$(T^*)_{13}$ and oligo$(A^*)_{13}$ were mixed in a 60 mM sodium cacodylate buffer (pH 7, 1 M NaCl, 100 mM $MgCl_2$; buffer A), very stable duplexes with a helix–coil transition temperature of 81 °C and an hypochromicity of 19% (at 1.2 μM single strand concentration) were obtained. This tendency of pyranosyl-like oligonucleotides to form stable complexes was demonstrated before with homo-DNA.[20] A transition temperature of 45 °C and a hypochromicity of 30% was observed for the single-strand oligo-$(T^*)_{13}$. This indicates the formation of hairpin structures or of

0947-6539/97/0301-0112 $ 15.00+.25/0 Chem. Eur. J. 1997, 3, No. 1

an oligo(T*)$_{13}$·oligo(T*)$_{13}$ duplex. The formation of intramolecular base pairing has been demonstrated before with oligo(α-thymidylate) sequences, but not with oligo(β-thymidylate).[33] In order to confirm duplex formation, the T_m values at different oligonucleotide concentrations in the aforementioned high-salt buffer were determined. The plot of T_m values versus oligomer concentration demonstrates that the T_m values increase linearly with increasing concentration (data not shown). These results are indicative for the intermolecular complex formation between oligo(T*)$_{13}$ strands,[34] which is in contrast to the results found for oligo(α-thymidylate). The T_m values and the hypochromicity observed by mixing equimolar amounts of oligo(T*)$_{13}$ with oligodeoxyadenylate are identical with the values observed for oligo(T*)$_{13}$ (Table 2, Figure 4A). It is not

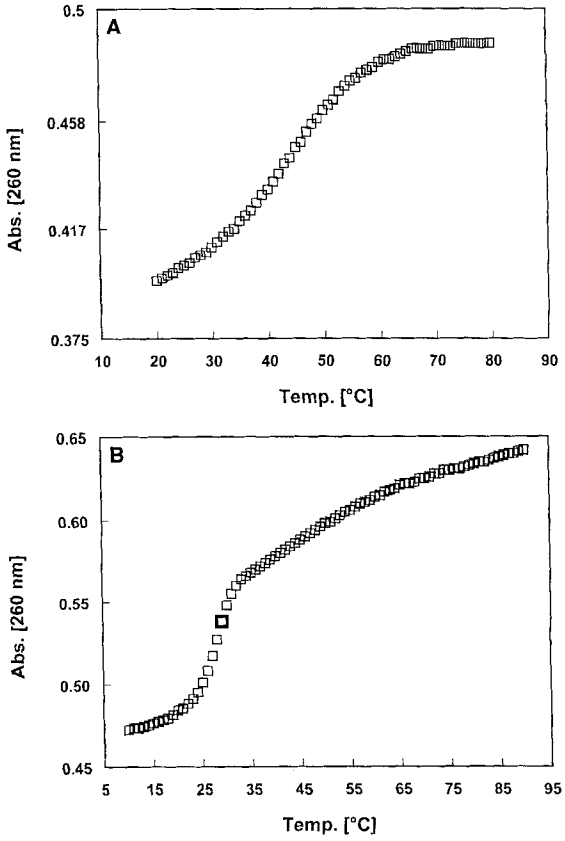

Fig. 4. Melting curve of A) oligo(T*)$_{13}$·oligo(dA)$_{13}$ and B) oligo(A*)$_{13}$·oligo(T)$_{13}$, both measured at 1 M NaCl, 60 mM cacodylate pH 7.0, 100 mM $MgCl_2$.

clear at this point whether the self-association of oligo(T*)$_{13}$ dominates the potential formation of oligo(T*)$_{13}$·oligodeoxyadenylate complexes in 1 M NaCl and 100 mM $MgCl_2$, so that formation of the latter complex cannot be observed, or whether both complexes have exactly the same T_m and hypochromicity.

As adenine–adenine pairing has been described in homo-DNA,[20] we investigated the thermal behaviour of oligo(A*)$_{13}$. However, we could not observe a cooperative melting behaviour below 90 °C. Only a linear increase in absorption with increasing temperature is observed, which might indicate the presence of an ordered single-strand structure.

By measuring the thermal stability of oligo(A*)$_{13}$·oligothymidylate mixtures (Figure 4B), we could observe for the first time the formation of complexes between a completely modified pyranose-like oligonucleotide and natural DNA. The observed melting point was found to be 30 °C and the hypochromicity 26% at 4 μM concentration of each strand. The relatively high hypochromicity indicates substantial base stacking. Apparently, the flexible oligothymidylate can adapt its conformation to the structure of the more rigid oligo(A*)$_{13}$. The second linear transition in the melting curve (Figure 4B) can be attributed to the thermal behaviour of the single-strand oligo(A*)$_{13}$ once the duplex is melted. The single-strand oligo(A*)$_{13}$, most probably, forms secondary structures, which disappear at higher temperature. The possibility of the first transition being due to triple-helix formation, however, can not be totally excluded based on these experiments. Nevertheless, a plot of T_m versus ln C shows an increase in the T_m as a function of the oligonucleotide concentration (Figure 5). This experiment excludes the formation of intramolecular hairpins and further sustains the hypothesis of the formation of intermolecular oligo(A*)$_{13}$·oligothymidylate complexes.

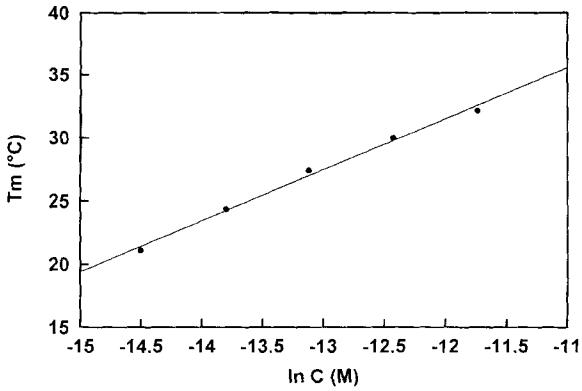

Fig. 5. T_m (°C) versus ln C (C in molarity) for the oligo(A*)$_{13}$·oligo(T)$_{13}$ duplex in 1 M NaCl, 60 mM Na cacodylate pH 7.0, 100 mM $MgCl_2$.

The data derived from the melting curve experiments were confirmed by CD measurements (Figure 6A). The CD spectra of oligo(T*)$_{13}$ and of an equimolar mixture of oligo(T*)$_{13}$ and oligodeoxyadenylate are similar (always at 1 M NaCl, 100 mM $MgCl_2$), which confirms the above-mentioned observations. Its similarity with the CD curve of oligonucleotide N3′ → P5′ phosphoramidates and with the A-form structure of ds RNA is striking.[35] Temperature-dependent CD measurements also confirm the T_m of 44 °C (45 °C for UV T_m determination) for the homoduplexes of oligo(T*)$_{13}$ (Figure 7A). A similar curve is obtained for the mixture of oligo(T*)$_{13}$ and oligodeoxyadenylate (Figure 7B); this result once more provides proof for the aforementioned hypothesis that the observed T_m corresponds to self-association of oligo(T*)$_{13}$. The ellipticity of the positive Cotton effect at 270 nm is temperature dependent and shifts to 277 nm with a decrease in intensity; an inflection point is observed at 45 °C. The very similar CD spectra of oligo(A*)$_{13}$ and of oligo(A*)$_{13}$·oligothymidylate (Figure 6A) sustain the hypothesis that oligothymidylate can adapt its structure to that of the rigid A* oligomer. The CD spectrum of oligo(A*)$_{13}$ is clearly

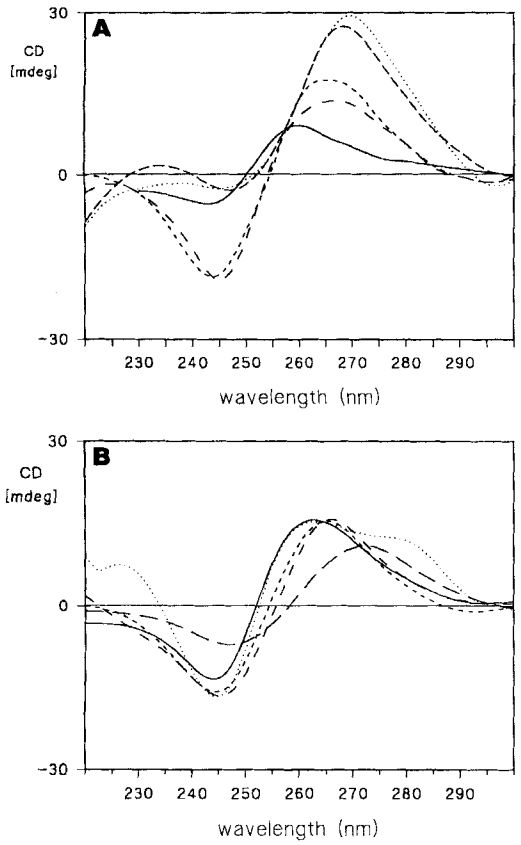

Fig. 6. CD spectra of the monomeric and duplex forms of the modified oligonucleotides, measured in: A) 1 M NaCl, 60 mM cacodylate, pH 7.0, 100 mM $MgCl_2$ (recorded at 10 °C); B) 0.1 M NaCl, 10 mM cacodylate, pH 7.0, 10 mM $MgCl_2$ (recorded at 30 °C, except oligo(A*)$_{13}$·oligo(T)$_{13}$ and oligo(A*)$_{13}$, which were recorded at 10 °C). oligo(T*)$_{13}$·oligo(A*)$_{13}$, ——; oligo(T*)$_{13}$·oligo(dA)$_{13}$, · · · ·; oligo(A*)$_{13}$·oligo(T)$_{13}$, – – –; oligo(T*)$_{13}$, — · — · —; oligo(A*)$_{13}$, - - - -.

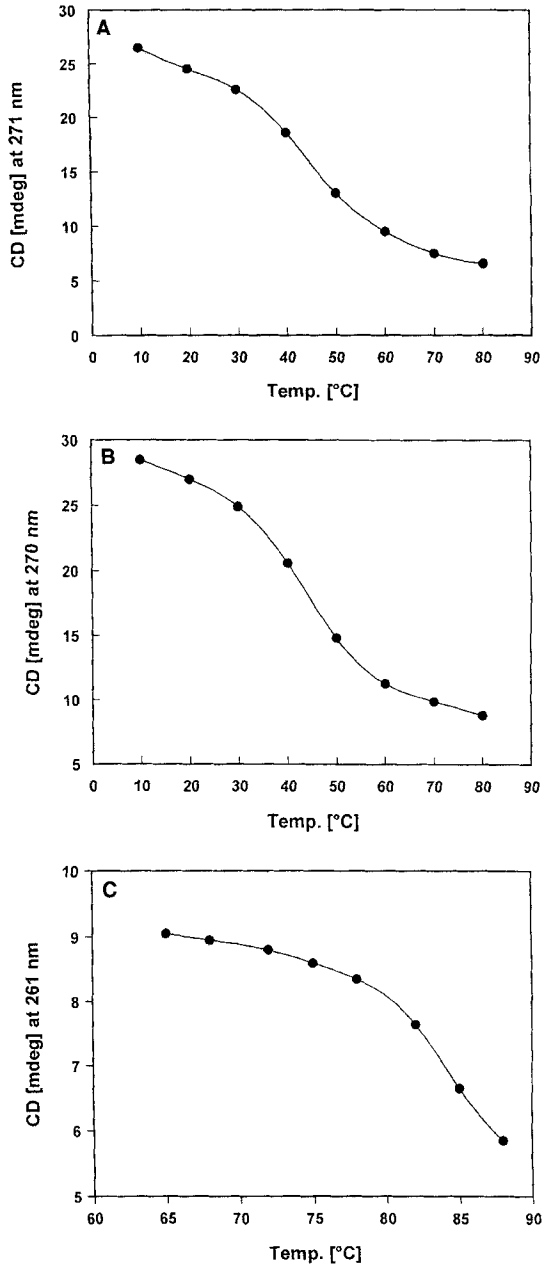

Fig. 7. Temperature-dependent CD measurements for A) oligo(T*)$_{13}$, B) oligo(T*)$_{13}$·oligo(dA)$_{13}$ and C) oligo(T*)$_{13}$·oligo(A*)$_{13}$ (measured in 1 M NaCl, 60 mM cacodylate, pH 7.0, 100 mM $MgCl_2$).

different from the spectrum of single-strand oligodeoxyadenylate.[36] The CD spectrum of the oligo(A*)$_{13}$·oligothymidylate complex shows a negative Cotton effect at 244 nm, and a positive Cotton effect at 265 nm and does not change substantially as a function of temperature. The temperature-dependent ellipticities $[\theta]$ of the B_{1u} and B_{2u} transition of oligo(A*)$_{13}$·oligothymidylate show a reversal point of the $[\theta](B_{2u})$ vs. T curve near the melting point (Figure 8). Several other transitions are visible, which suggest that other transformations are taking place. The technique, however, does not allow conclusions concerning these secondary interactions. The CD spectrum of the oligo(T*)$_{13}$·oligo(A*)$_{13}$ (Figure 6A) duplex is different from the spectrum of the natural oligodeoxythymidylate·oligodeoxyadenylate duplex.[37, 38] The T_m value of 81 °C is confirmed by the temperature-dependent CD measurements (Figure 7C).

It should be mentioned that the T_m values given above were determined at a salt concentration of 1 M NaCl in the presence of 100 mM $MgCl_2$. High salt concentrations stabilise oligonucleotide duplexes by an entropically more favourable counterion condensation.[39] Because this salt concentration is higher than under physiological conditions, T_m measurements were repeated in 0.1 M NaCl (10 mM $MgCl_2$, 10 mM Na cacodylate buffer, pH 7), and the results are summarised in Table 2, column B. The duplex composed of oligo(T*)$_{13}$·oligo(A*)$_{13}$ has a similar T_m to that at high salt concentration. These data are confirmed by

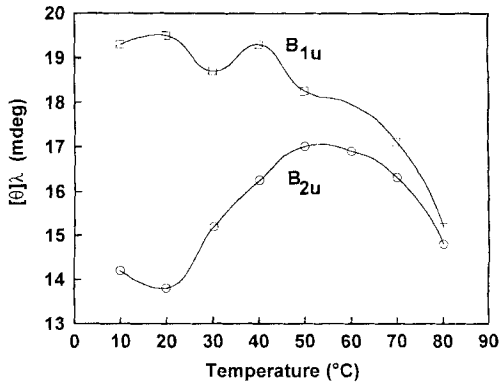

Fig. 8. Temperature-dependent ellipticities of the B_{1u} and B_{2u} transitions of the CD spectra of oligo(A*)$_{13}$·oligo(T)$_{13}$, measured in 1 M NaCl, 60 mM cacodylate, pH 7.0, 100 mM $MgCl_2$.

0947-6539/97/0301-0114 $ 15.00+.25/0 Chem. Eur. J. 1997, 3, No. 1

temperature-dependent CD measurements (data not shown). As expected, the duplex between oligo(T)$_{13}$ and oligo(A*)$_{13}$ is less stable at low salt concentrations. Single-strand oligo(T*)$_{13}$ and single-strand oligo(A*)$_{13}$ do not show a tendency to self-associate at low salt concentrations; neither a UV melting point, nor a CD melting point is observed. This result contrasts with the self-association of oligo(T*)$_{13}$ at high salt concentration. It is known that, by changing salt concentration, structural transitions occur in DNA, and this is here clearly the case here. The formation of oligo(T*)$_{13}$ homoduplexes is favoured at high (1 M NaCl), but not at lower (0.1 M NaCl) salt concentrations. The absence of oligo(T*)$_{13}$·oligo(T*)$_{13}$ duplex formation at low salt concentration is incontrovertible proof for the existence of oligo(T*)$_{13}$·oligo(dA)$_{13}$ complexes. The T_m of this duplex, however, is higher (60 °C) than the T_m observed at high salt concentration (45 °C); this further confirms the proposal that the association observed at high salt concentration are oligo(T*)$_{13}$·oligo(T*)$_{13}$ interactions.

The CD spectra measured at 0.1 M NaCl (Figure 6B) are clearly different from those measured at 1 M NaCl (Figure 6A). The CD spectra of oligo(A*)$_{13}$, of oligo(A*)$_{13}$·oligo(T)$_{13}$ and of oligo(A*)$_{13}$·oligo(T*)$_{13}$ are similar (Figure 6B), showing a negative Cotton effect around 245 nm and a positive Cotton effect around 265 nm. These spectra are also similar to the CD spectra of oligo(A*)$_{13}$ and oligo(A*)$_{13}$·oligothymidylate at high salt concentration (Figure 6A). At 0.1 M NaCl concentration, however, the CD spectra of the heterocomplex formed between oligoadenylate and oligo(T*)$_{13}$ and of oligo(T*)$_{13}$ alone are different from each other, while at 1.0 M NaCl concentration both spectra are similar; this again suggests the absence of oligo(T*)$_{13}$·oligo(dA)$_{13}$ duplex formation and the presence of oligo(T*)$_{13}$·oligo(T*)$_{13}$ interactions at high salt concentration.

An intriguing phenomenon is the difference in results obtained in 1 M NaCl/100 mM $MgCl_2$/60 mM Na cacodylate buffer and the 0.1 M NaCl/10 mM $MgCl_2$/10 mM Na cacodylate buffer for the oligo(T*)$_{13}$·oligo(T*)$_{13}$ and oligo(T*)$_{13}$·oligo(dA)$_{13}$ mixtures. Therefore, experiments were repeated under different conditions, initially in 0.1 M NaCl/0.02 M potassium phosphate buffer with and without the addition of 10 mM $MgCl_2$ (summarised in Table 2, columns C and D). The results obtained with buffer C do not demonstrate essential differences in the thermal behaviour of the different oligonucleotides, except for oligo(T*)$_{13}$·oligo(dA)$_{13}$. Also here neither oligo(A*)$_{13}$ nor oligo(T*)$_{13}$ show a tendency to form homoduplexes, although single-strand oligo(A*)$_{13}$ and oligo(T*)$_{13}$ show an ordered structure. This is demonstrated by the more or less linear increase in the UV absorption with temperature, both for oligo(A*)$_{13}$ and oligo(T*)$_{13}$. An equimolar mixture of oligo(T*)$_{13}$ and oligodeoxyadenylate shows a melting temperature of 45 °C with a hypochromicity of 49% when measured at 284 nm, possibly indicating triple-helix formation. The thermal behaviour of the complex at 260 nm, however, shows a distorted curve.[40] At 260 nm, the absorbance first decreases, showing a minimum at 46 °C (the melting point observed at 284 nm), and then increases to a second transition at 58 °C (Figure 9A).

Deviations from normal melting curves have also been observed with telomeric sequences, but the nature of this interaction is not completely resolved.[41] Because triple-helix formation is demonstrated more easily in the presence of $MgCl_2$, we repeated the melting point experiments in buffer D (Table 2, column D). T_m values for oligo(T)$_{13}$·oligo(A*)$_{13}$ and oligo(T*)$_{13}$·oligo(A*)$_{13}$ were similar to those previously observed with the other buffers. However, it is remarkable that with buffer D the same melting curves were obtained at 260 and 284 nm, whereas for the natural oligo(dA)$_{13}$·oligo(T)$_{13}$ duplex a transition was only visible at 260 nm and not at 284 nm. Under these conditions the mixture of oligo(T*)$_{13}$ and oligo(dA)$_{13}$ gave a melting curve at 260 nm with three distinct transitions (Figure 9B), indicating duplex and triple-helix formation. At 284 nm only one transition could be observed at 53 °C, presumably the melting point for the oligo(T*)$_{13}$·oligo(dA)$_{13}$·oligo(T*)$_{13}$ triplex. This leads to the conclusion that the T_m observed at 71 °C (260 nm) corresponds to the melting point of the oligo(T*)$_{13}$·oligo(dA)$_{13}$ duplex. The smaller transition observed at 39 °C cannot be explained, but might be assigned to oligo(T*)$_{13}$·oligo(T*)$_{13}$ interactions.

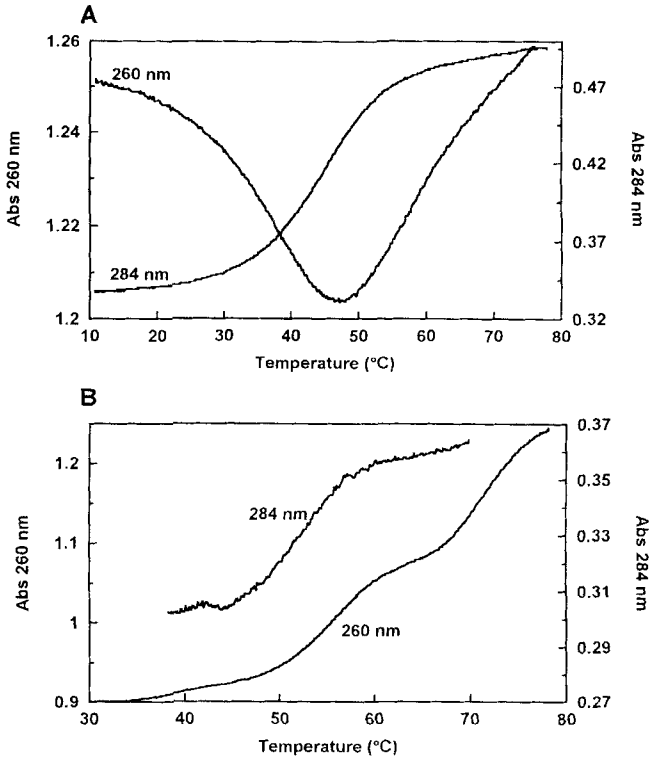

Fig. 9. Melting curves of oligo(T*)$_{13}$·oligo(dA)$_{13}$ measured at 260 and 284 nm in A) 0.1 M NaCl, 0.02 M KH_2PO_4, pH 7.5, 0.1 mM EDTA and B) the same buffer with addition of 10 mM $MgCl_2$.

The melting temperatures of the oligo(T*)$_{13}$·oligo(dA)$_{13}$ duplex and of oligo(T*)$_{13}$ were then determined in 1 M NaCl in the absence of $MgCl_2$ (Table 3, buffers E and F). In both buffers oligo(T*)$_{13}$ homoduplexes are formed as well as oligo(T*)$_{13}$·oligo(dA)$_{13}$ duplexes. The latter duplex could not be observed in the buffer A (buffer F with 100 mM $MgCl_2$), even though in buffers E and F the T_m of the oligo(T*)$_{13}$·oligo(dA)$_{13}$ duplex is considerably higher than the T_m of the oligo(T*)$_{13}$ homoduplexes. Apparently heteroduplex formation between oligo(T*)$_{13}$ and oligodeoxyadenylate is prevented in the presence of $MgCl_2$ combined with a high salt concentration. Unfortunately, addition of $MgCl_2$ to buffer E resulted in a precipita-

  0947-6539/97/0301-0115 $ 15.00+.25/0

Table 3. T_m (°C) observed for oligo(T*)$_{13}$·oligo(dA)$_{13}$ and for oligo(T*)$_{13}$ in different buffer media, measured at both 260 and 284 nm.

Buffer		oligo(T*)$_{13}$·oligo(dA)$_{13}$ (4 μM each)	oligo(T*)$_{13}$ (8 μM)
A	1 M NaCl, 60 mM Na cacodylate pH 7.0, 100 mM $MgCl_2$	45.0 [a]	45.0
E	1 M NaCl, 0.02 M KH_2PO_4 pH 7.5, 0.1 mM EDTA	64.8	48.0
F	1 M NaCl, 60 mM Na cacodylate pH 7.0	67.0	50.0

[a] Melting point observed is that of the oligo(T*)$_{13}$·oligo(T*)$_{13}$ duplex.

tion so that these experimental conditions could not be investigated.

In order to be able to evaluate base pairing in completely modified oligonucleotides, mixed sequences containing only anhydrohexitol nucleosides were synthesised. Fully modified homopurine sequences containing the adenine (A*) and guanine (G*) nucleoside analogues were evaluated. Two hexamer sequences and a dodecamer (Table 4) were synthesised, and the scrambled sequences were chosen so as to avoid a possible self-complementary recognition by A*–G* base pairs. All these fully modified sequences and their control sequences were prepared on a 1,3-propanediol-containing support, which obviated the need to prepare succinates of the modified nucleoside analogues. The extra 3′-(3-hydroxypropyl)phosphodiester moiety has no influence on melting temperatures, as was previously shown for other constructs in our laboratory.[42] However, phosphodiesterase activity with such oligomers is significantly reduced.[42, 43]

Table 4. Melting temperatures of fully modified hexamers and dodecamers determined in 0.1 M NaCl, 20 mM KH_2PO_4, pH 7.5, 0.1 mM EDTA. Duplexes were formed with the complementary sequences 5′-TCTCCT (for **7** and **8**), 5′-TCTCTC (for **9** and **10**) and 5′-TCTCCTCTCCCT (for **11** and **12**) (DNA complement); 5′-TT-r(UCUCCU)-TT (for **7** and **8**), 5′-TT-r(UCUCUC)-TT (for **9** and **10**) and 5′-TT-r(UCUCCUCUCCCU)-TT (for **11** and **12**) (RNA complement). The higher salt concentration was necessary for the hexamers with DNA as the complement, since otherwise no duplex could be detected for **8** and **10**.

Sequence (4 μM equimolar mixture with complement)		T_m (°C) DNA compl.	T_m (°C) RNA compl.
7	6′-A*G*G*A*G*A*	31.2 [a]	44.8
8	5′-AGGAGA	10.0 [a]	ND [b]
9	6′-G*A*G*A*G*A*	14.7 [a]	42.8
10	5′-GAGAGA	9.5 [a]	ND [b]
11	6′-A*G*G*G*A*G*A*G*G*A*G*A*	64.8	84.0
12	5′-AGG GAG AGG AGA	49.0	47.6

[a] Determined at 1 M NaCl. [b] ND: not determined due to the low melting temperature.

It was unlikely that all three possible purine pairs would exist, but to be absolutely sure, we studied the thermal denaturation profiles of the single-strand sequences as well. Only a linear increase in UV absorbance was observed, corresponding to classical destacking of the bases of a single-strand oligonucleotide upon heating.

Thermal denaturation of the hexamers with their DNA complement was studied in 1 M NaCl (containing 20 mM KH_2PO_4, pH 7.5, and 0.1 mM EDTA). The most important phenomenon is the clear formation of a duplex between the hexitol oligonucleotides and their natural counterparts. Moreover, these modified duplexes are more stable than the control duplexes consisting exclusively of natural nucleotides.

It is striking, however, that there is a large difference in melting temperature for sequences **7** (T_m = 31.2 °C) and **9** (T_m = 14.7 °C) (Table 4) with their antiparallel complementary oligonucleotides. Although both modified oligonucleotides contain 3 G* and 3 A* residues differing only in their sequence order, the melting temperature for **7** is double that for **9**. This sequencedependent effect is only weakly reflected by the control oligonucleotides **8** and **10**.

Looking at the dodecamers (T_m determined at 0.1 M NaCl) one again notices an increased stability of the fully modified oligonucleotide **11** compared to its control sequence **12** with an increase in melting temperature of 16 °C. The formation of complexes between a completely modified hexitol-like oligonucleotide and natural oligonucleotides is remarkable, especially given the increased stability compared to the natural Watson–Crick duplexes.

As antisense oligonucleotides are primarily targeted against RNA, we repeated T_m determination of the corresponding RNA–HNA (hexitol nucleic acids) duplexes in 0.1 M NaCl. The T_m of the hexameric and dodecameric RNA–HNA duplexes are substantially higher than those of the DNA–HNA duplexes (Table 4). The increase in T_m for the dodecamer (in comparison with the natural DNA–RNA duplex) is 36.4 °C, which means a ΔT_m of 3 °C per base pair. It is striking that the sequence dependency of the T_m is lower for the RNA–HNA duplex than for the DNA–HNA duplex.

For the fully modified mixed dodecamer **11** the influence of one or two identical mismatches on the stability of a duplex formed with its DNA complement was investigated and compared with the results obtained for a DNA–DNA duplex containing the same mismatches (Table 5). The melting behaviour was examined in a buffer containing 0.1 M NaCl, 20 mM KH_2PO_4, pH 7.5, 0.1 mM EDTA. The mismatches were located

Table 5. Influence of mismatches towards G* and A* on the melting temperature (C, at 260 nm) of HNA–DNA duplexes determined in 0.1 M NaCl, 20 mM KH_2PO_4, pH 7.5, 0.1 mM EDTA; concentration of each oligonucleotide, 4 μM.

		HNA–DNA 6′-(AGG GAG AGG AGA)* 3′-TCC *CTC TCC* TCT-5′ *xy* *xy yx*		DNA–DNA 5′-AGG GAG AGG AGA-3′ 3′-TCC *CTC TCC* TCT-5′ *xy* *xy yx*	
x	*y*	T_m (°C)	ΔT_m (°C)	T_m (°C)	ΔT_m (°C)
control		65.2	–	49.4	–
1 × G		49.8	−15.4	37.0	−12.4
1 × A		47.9	−17.3	37.8	−11.6
1 × T		55.0	−10.2	35.4	−14.0
2 × G		32.7	−32.5	27.5	−21.9
2 × A		28.5	−36.7	28.8	−20.6
2 × T		46.8	−18.4	24.0	−25.4
	1 × G	44.9	−20.3	35.9	−13.5
	1 × A	54.3	−10.9	38.0	−11.4
	1 × C	56.2	−9.0	34.3	−15.1
	2 × G	41.8	−23.4	35.5	−13.9
	2 × A	41.8	−23.4	24.4	−25.0
	2 × C	48.4	−16.8	21.0	−28.4

0947-6539/97/0301-0116 $ 15.00+.25/0 Chem. Eur. J. 1997, 3, No. 1

in the middle of the sequence. It can be seen from Table 5 that the discrimination of the HNA dodecamer towards the different sequences is very high; this indicates that HNA has a very strong potential for selective inhibition of a target in antisense strategy.

Electrophoretic Behaviour and Enzymatic Stability: The formation of oligo(T*)$_{13}$·oligo(dA)$_{13}$ and oligo(A*)$_{13}$·oligo(T)$_{13}$ duplexes is supported by electrophoretic mobility data. Because of difficulties with ^{32}P end-labelling of the 1′,5′-anhydrohexitol nucleosides by means of T4 polynucleotide kinase, an electrophoretic assay was performed using a titration experiment as described by Cooney et al.[44] The natural dA and T 13-mers were ^{32}P-labelled and then titrated with unlabelled oligo(A*)$_{13}$ and oligo(T*)$_{13}$. The outcome of such a titration experiment is shown in Figure 10, assayed on a 20% nondenaturing polyacryl-

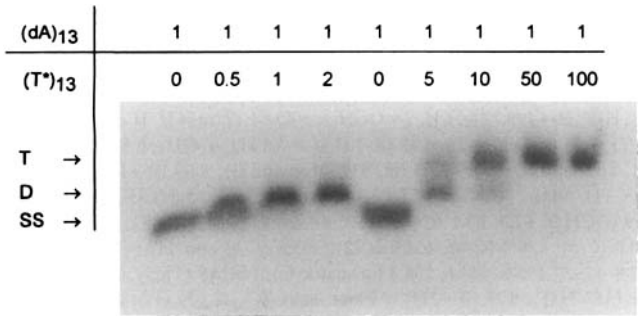

Fig. 10. Nondenaturing polyacrylamide gel electrophoresis of radiolabelled oligo(dA)$_{13}$ and different amounts of oligo(T*)$_{13}$ (SS = single strand, D = duplex, T = triplex).

amide gel.[45] The single-strand oligo(dA)$_{13}$ is in lane 1. Upon addition of an equimolar amount of oligo(T*)$_{13}$ a new band with lower mobility was observed. This band corresponds to the oligo(T*)$_{13}$·oligo(dA)$_{13}$ duplex, which migrates more slowly through the gel matrix. Binding of a second oligo(T*)$_{13}$ to form an oligo(T*)$_{13}$·oligo(dA)$_{13}$·oligo(T*)$_{13}$ triplex was observed at an oligo(T*)$_{13}$:oligo(dA)$_{13}$ ratio of 5:1. The presence of exclusive triplexes was observed at a ratio of 50:1. Formation of the duplex oligo(A*)$_{13}$·oligo(T)$_{13}$ could not be detected by gel electrophoresis; this might be due to the fact that this duplex is less stable or that the oligo(A*)$_{13}$·oligo(T)$_{13}$ duplex co-migrates with the radiolabelled oligo(T)$_{13}$. Co-migration was also observed for the natural oligo(dA)$_{13}$·oligo(T)$_{13}$ duplex, which was nevertheless well separated from the radiolabelled oligo(dA)$_{13}$ (data not shown).

A major requirement that must be met by antisense oligonucleotides is their stability towards enzymatic degradation under assay conditions and in vivo. Natural oligonucleotides are unstable and need to be stabilised towards nucleases by chemical modification or physical separation from the medium, for example, by incorporation into liposomes. As it is known that 3′-exonuclease activity is the major cause of degradation of oligonucleotides in serum,[46] it seemed suitable to study the stability of our chemically modified oligonucleotides in the presence of snake venom phosphodiesterase (SVPDE, a 3′-exonuclease).

During digestion with SVPDE, the increase in absorbance (hyperchromicity) at 260 nm was followed.[22] Fitting of the data obtained to an exponential curve resulted in the half-lives indicated in the legend of Figure 11. While oligodeoxyadenylate

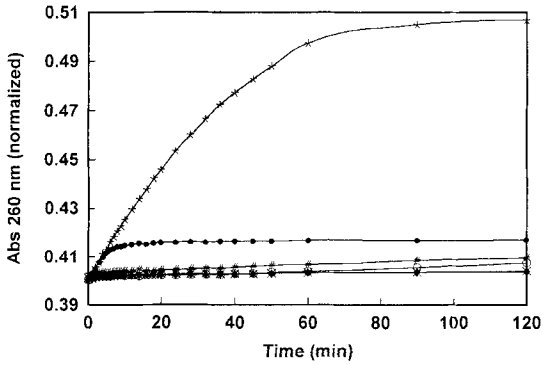

Fig. 11. Digestion of oligonucleotides (T)$_{13}$, (T*)$_{13}$, (T*)$_2$(T)$_9$(T*)$_2$, (dA)$_{13}$, (A*)$_{13}$ and (A*)$_2$(dA)$_9$(A*)$_2$ with snake venom phosphodiesterase. ● = (T)$_{13}$, $t_{1/2}$ = 4 min; * = (dA)$_{13}$, $t_{1/2}$ = 24 min; # = (T*)$_2$(T)$_9$(T*)$_2$, $t_{1/2}$ > 120 min; ○ = (A*)$_2$(dA)$_9$(A*)$_2$, $t_{1/2}$ > 120 min; ♦ = (T*)$_{13}$, × = (A*)$_{13}$; (T*)$_{13}$ and (A*)$_{13}$ were completely stable under reaction conditions.

is degraded very fast ($t_{1/2}$ = 24 min), oligo(A*)$_{13}$ is completely stable towards SVPDE. No change in absorption could be detected, not even after 24 hours. Substitution with two adenine anhydrohexitol nucleosides (A*) at either end of an oligonucleotide, likewise provides constructs of high stability. These results were confirmed with oligonucleotides containing thymine anhydrohexitol analogues (T*).

Conclusion

Hexitol nucleic acids (HNA) form very stable self-complementary duplexes as well as stable duplexes with their natural counterparts. These hybridisation characteristics are dependent on the base sequence and the experimental conditions. At high salt concentration oligo(T*)$_{13}$·oligo(T*)$_{13}$ duplexes are formed, but not at low salt concentration. Triple-helix formation can be observed with oligo(T*)$_{13}$ and oligo(dA)$_{13}$, but this complex formation is highly dependent on the experimental conditions. CD experiments suggest a DNA–HNA duplex structure closely resembling the A-form structure of ds RNA. A ΔT_m of 3 °C per base pair has been observed for homopurine RNA–HNA duplexes. With regard to their structure, this can be explained by the almost identical distance between the 3′- and 5′-phosphodiester residues in the hexitol and in the deoxy-β-D-ribofuranosyl oligonucleotides and by the axial position of the bases of the hexitol nucleosides. A mixed HNA purine dodecamer displays very strong and selective base pairing and discriminates clearly between matched and mismatched sequences. Oligonucleotides containing one or more 1′,5′-anhydrohexitol residues show high phosphodiesterase stability towards degradation by snake venom phosphodiesterase. Like PNA and xylose-DNA, this is another example of a completely new backbone for the construction of oligonucleotide analogues making base pairs with their natural antiparallel complementary sequence. Moreover, these

oligonucleotides are highly soluble in aqueous medium, in contrast to nonionic oligomers. These observations may hold great promise for the use of hexitol oligonucleotides as antisense drugs.

Experimental Procedure

Ultraviolet spectra were recorded with a Philips PU 8740 UV/Vis spectrophotometer. The ^{1}H and ^{13}C NMR spectra were determined with a JEOL FX90Q spectrometer with tetramethylsilane as internal standard for the ^{1}H NMR spectra, and [D$_6$]DMSO ($\delta = 39.6$) or $CDCl_3$ ($\delta = 76.9$) for the ^{13}C NMR spectra (s = singlet, d = doublet, dd = doublet of doublets, t = triplet, brs = broad signal, m = multiplet). Chemical ionisation mass spectra (CIMS) and liquid secondary ion mass spectra (LSIMS) were obtained using Kratos Concept ^{1}H mass spectrometer. Precoated Machery-Nagel Alugram® Sil G/UV 254 plates were used for TLC, and the spots were examined with UV light and sulfuric acid–anisaldehyde spray. Column chromatography was performed on Janssen Chimica silica gel (0.060–0.200 nm). Anhydrous solvents were obtained as follows: dichloromethane was stored over calcium hydride, refluxed and distilled; pyridine, triethylamine and *N,N*-diisopropylethylamine were refluxed overnight over potassium hydroxide and distilled. *n*-Hexane and acetone, used in the purification of the phosphoramidites, were purified by distillation.

1,5-Anhydro-2,3-dideoxy-2-(thymin-1-yl)-D-*arabino*-hexitol (6a): Alkylation of N^3-benzoylthymine with 1,5-anhydro-4,6-*O*-benzylidene-3-deoxy-D-glucitol under Mitsunobu reaction conditions yielded **6a** after deprotection, as described previously [26]. ^{1}H NMR ([D$_6$]DMSO): $\delta = 1.77$ (s, CH_3), 1.6–2.5 (m, 2H, H-3′, H-3″), 3.05–3.30 (m, 1H, H-5′), 3.4–4.1 (m, 4H) and 3.7–4.1 (m, 2H, H-1′, H-1″, H-4′, H-6′, H-6″), 4.52 (m, 1H, H-2′), 4.65 (t, $J = 5.7$ Hz, 6′-OH), 4.89 (d, $J = 5$ Hz, 4′-OH), 7.88 (s, H-6), 11.25 (br, NH); ^{13}C NMR ([D$_6$]DMSO): $\delta = 12.3$ (CH_3), 35.2 (C-3′), 50.1 (C-2′), 60.3, 60.8 (C-4′, C-6′), 66.9 (C-1′), 82.4 (C-5′), 108.3 (C-5), 138.9 (C-6), 150.9 (C-2), 163.8 (C-4); UV (MeOH): λ_{max} (ε) = 272 nm (9500); CIMS (iC_4H_{10}) *m/z*: 257 $[M+H]^+$, 127 $[B+2H]^+$; Elem. anal. ($C_{11}H_{16}N_2O_5$): calculated C: 51.56, H: 6.29, N: 10.93; found C: 51.40, H: 6.24, N: 10.87.

1,5-Anhydro-2-(N^6-benzoyladenin-9-yl)-2,3-dideoxy-D-*arabino*-hexitol (6b): To a solution of 1,5-anhydro-4,6-*O*-benzylidene-2-(adenin-9-yl)-2,3-dideoxy-D-*arabino*-hexitol [26] (2.3 g, 6.51 mmol) in dry pyridine (100 mL) was added benzoyl chloride (0.9 mL, 7.8 mmol) at 0 °C. After having been stirred for 4 h at room temperature, the mixture was cooled on an ice bath and H_2O (2 mL) was added. After addition of concentrated NH_3 solution (1.5 mL, 33%) and further stirring for 45 min at room temperature, the mixture was evaporated. The residue was purified by column chromatography (CH_2Cl_2–MeOH, 98:2) affording 1.92 g (4.19 mmol) of 1,5-anhydro-4,6-*O*-benzylidene-2-(N^6-benzoyladenin-9-yl)-2,3-dideoxy-D-*arabino*-hexitol as colourless foam (64%). This was further treated with 80% acetic acid (100 mL) at 60 °C for 5 h to remove the benzylidene moiety. Evaporation, coevaporation with toluene and purification by column chromatography (CH_2Cl_2–MeOH, 95:5 to 90:10) afforded a colourless foam (1.10 g, 2.98 mmol, 71%). ^{1}H NMR ([D$_6$]DMSO): $\delta = 1.94$ (m, 1H, H-3′ax), 2.32 (m, 1H, H-3′eq), 3.21 (m, 1H, H-5′), 3.42–3.76 (m, 3H, H-4′, H-6′, H-6″), 3.90 (dd, $^2J = 13$ Hz, 1H, H-1′ax), 4.27 (dd, $^2J = 12.2$ Hz, 1H, H-1′eq), 4.67 (t, $J = 5.7$ Hz, 1H, 6′-OH), 4.88–5.00 (m, 2H, H-2′, 4′-OH), 7.47–7.68 (m, 3H, aromatic H), 8.00–8.07 (m, 2H, aromatic H), 8.60 (s, 1H), 8.73 (s, 1H, H-2, H-8), 11.0 (brs, 1H, NH); ^{13}C NMR ([D$_6$]DMSO): $\delta = 35.8$ (C-3′), 50.7 (C-2′), 60.5, 60.7 (C-4′, C-6′), 67.9 (C-1′), 83.1 (C-5′), 125.1 (C-5), 128.5 (*o*-C, *m*-C), 132.5 (*p*-C), 133.6 (Cx), 143.5 (C-8), 150.3 (C-4), 151.4 (C-2), 152.4 (C-6), 164.5 (C=O); UV (MeOH): λ_{max} (ε) = 282 nm (20200); LSIMS (Thgly, NaOAc) *m/z*: 392 $[M+Na]^+$, 370 $[M+H]^+$, 240 $[B+2H]^+$; Elem. anal. ($C_{18}H_{19}N_5O_4$): calculated C: 58.53, H: 5.18, N: 18.96; found C: 58.42, H: 4.98, N: 18.72.

1,5-Anhydro-2,3-dideoxy-2-(N^2-isobutyrylguanin-9-yl)-D-*arabino*-hexitol (6c): Alkylation of N^2-isobutyryl-O^6-[2-(*p*-nitrophenyl)ethyl]guanine (1.85 g, 7.5 mmol) with 1,5-anhydro-4,6-*O*-benzylidene-3-deoxy-D-glucitol [26] (1.18 g, 5 mmol) yielded, after removal of the *p*-nitrophenylethyl group with DBU (1.5 mL, 10 mmol) in anhydrous pyridine for 16 h and purification by flash column chromatography (CH_2Cl_2–MeOH, 99:1 to 97:3), 1.35 g of crude 1,5-anhydro-4,6-*O*-benzylidene-2,3-dideoxy-2-(N^2-isobutyryl-O^6-[2-(*p*-nitrophenyl)ethyl]guanin-9-yl)-D-*arabino*-hexitol. Hydrolysis of the benzylidene moiety with 80% HOAc (100 mL, 5 h at 60 °C) gave, after column chromatography (CH_2Cl_2–MeOH, 90:10), compound **6c** as a colourless foam (610 mg, 1.74 mmol, 34% overall yield). ^{1}H NMR ([D$_6$]DMSO): $\delta = 1.11$ (d, $J = 6.7$ Hz, 6H, CH_3), 1.93 (m, 1H, H-3′ax), 2.11–2.38 (m, 1H, H-3′eq), 2.80 (m, 1H, C*H*Me$_2$), 3.25 (m, 1H, H-5′), 3.42–3.78 (m, 3H, H-4′, H-6′, H-6″), 3.89 (dd, $^2J = 13$ Hz, 1H, H-1′), 4.21 (dd, $^2J = 13$ Hz, 1H, H-1″), 4.69 (t, $J = 5.2$ Hz, 1H, 6′-OH), 4.81 (m, 1H, H-2′), 4.97 (d, $J = 5.1$ Hz, 1H, 4′-OH), 8.39 (s, 1H, H-8), 10.41 (s, 1H, NH); ^{13}C NMR ([D$_6$]DMSO): $\delta = 19.4$ (CH_3) 34.5 (*C*HMe$_2$), 35.8 (C-3′), 50.5 (C-2′), 60.5, 60.7 (C-4′, C-6′), 67.9 (C-1′), 83.1 (C-5′), 116.7 (C-5), 141.7 (C-8), 152.0 (C-4), 153.0 (C-2), 159.8 (C-6), 175.2 (C=O); UV (MeOH): λ_{max} 273 nm; LSIMS (Thgly, NaOAc) *m/z*: 352 $[M+H]^+$; Elem. anal. ($C_{15}H_{21}N_5O_5$): calculated C: 51.28, H: 6.02, N: 19.93; found C: 51.17, H: 5.97, N: 19.72.

1,5-Anhydro-2,3-dideoxy-6-*O*-dimethoxytrityl-2-(thymin-1-yl)-D-*arabino*-hexitol (7a): Dimethoxytrityl chloride (480 mg, 1.42 mmol) was added to **6a** (330 mg, 1.29 mmol) dissolved in anhydrous pyridine (20 mL). The mixture was stirred overnight at room temperature, diluted with CH_2Cl_2 (100 mL) and washed twice with saturated aqueous $NaHCO_3$ solution (100 mL). The organic layer was dried, evaporated, and coevaporated with toluene. The resulting residue was purified by column chromatography (with a gradient of 0 to 3% MeOH in $CHCl_3$ containing 1% triethylamine) to yield the title compound as a colourless foam (373 mg, 0.67 mmol, 52%). ^{1}H NMR ($CDCl_3$): $\delta = 1.60–2.50$ (m, 2H, H-3′, H-3″), 1.91 (s, 3H, CH_3), 3.12–3.62 (m, 2H, H-5′, H-4′), 3.77 (s, 6H, 2 × OCH_3), 3.65–4.17 (m, 4H, H-6′, H-6″, H-1′, H-1″), 4.53 (s, 1H, H-2′), 4.88 (d, 1H, $J = 5.1$ Hz, 4′-OH), 6.81 (d, $J = 8.7$, 4H, aromatic H), 7.09–7.53 (m, 9H, aromatic H), 8.09 (s, 1H, H-6), 9.10 (brs, 1H, NH); ^{13}C NMR ($CDCl_3$): $\delta = 12.5$ (CH_3), 35.5 (C-3′), 50.7 (C-2′), 54.9 (OCH_3), 62.4, 63.1 (C-4′, C-6′), 68.2 (C-1′), 81.1 (C-5′), 86.0 (Ph_3C), 110.0 (C-5), 138.4 (C-6), 151.0 (C-2), 163.8 (C-4) and 112.9, 126.6, 127.5, 127.8, 129.7, 135.6, 144.6, 158.3 (aromatic C); LSIMS (Thgly, NaOAc) *m/z*: 581 $[M+Na]^+$, 127 $[B+2H]^+$; Elem. anal. ($C_{32}H_{34}N_2O_7$): calculated C: 68.80, H: 6.13, N: 5.01; found C: 68.91, H: 6.07, N: 4.80.

1,5-Anhydro-2-(N^6-benzoyladenin-9-yl)-2,3-dideoxy-6-*O*-dimethoxytrityl-D-*arabino*-hexitol (7b): A solution of the nucleoside **6b** (370 mg, 1 mmol) and of 4,4′-dimethoxytrityl chloride (400 mg, 1.2 mmol) in dry pyridine (25 mL) was stirred at room temperature for 16 h. The mixture was diluted with CH_2Cl_2 (100 mL) and washed twice with saturated aqueous $NaHCO_3$ solution (100 mL). The organic layer was dried, evaporated and coevaporated with toluene. The residue was purified by column chromatography (0 to 3% of MeOH in CH_2Cl_2 containing 0.2% of pyridine) to obtain a colourless foam (400 mg, 0.6 mmol, 63%). ^{1}H NMR ($CDCl_3$): $\delta = 1.75–2.45$ (m, 2H, H-3′, H-3″), 3.18–4.22 (m, 12H, H-4′, H-5′, H-6′, H-6″, H-1′, H-1″; s at 3.78, 2 × OCH_3), 4.88–5.00 (d and s, $J = 5$ Hz, 2H, H-2′, 4′-OH), 6.65–6.92 (m, 4H, aromatic H), 7.23 (m, 9H, aromatic H), 7.45–7.65 (m, 3H, aromatic H), 7.99–8.05 (m, 2H, aromatic H), 8.54 (s, 1H), 8.76 (s, 1H), (H-2, H-8), 9.12 (brs, 1H, NH); ^{13}C NMR ($CDCl_3$): $\delta = 35.7$ (C-3′), 50.6 (C-2′), 55.1 (OCH_3), 60.5, 60.7 (C-4′, C-6′), 67.8 (C-1′), 83.1 (C-5′), 86.7 (Ph_3C), 122.9 (C-5), 128.7 (Bz), 132.5 (Bz), 133.8 (Bz), 143.6 (C-8), 149.4 (C-4), 152.2, 152.4 (C-2, C-6), 165.6 (C=O) and 113.1, 126.7, 127.8, 127.9, 129.8, 135.7, 135.9, 144.5, 158.5 (aromatic C, Tr); LSIMS (Thgly, NaOAc) *m/z*: 694 $[M+Na]^+$, 240 $[B+2H]^+$ Elem. anal. ($C_{39}H_{37}N_5O_6$): calculated C: 69.73, H: 5.55, N: 10.43; found C: 69.91, H: 5.71, N: 10.22.

1,5-Anhydro-2,3-dideoxy-6-*O*-dimethoxytrityl-2-(N^2-isobutyrylguanin-9-yl)-D-*arabino*-hexitol (7c): A solution of the nucleoside **6c** (580 mg, 1.65 mmol) and dimethoxytrityl chloride (670 mg, 2.0 mmol) in anhydrous pyridine (20 mL) was stirred at room temperature for 16 h. The mixture was diluted with CH_2Cl_2 (100 mL) and washed twice with a saturated aqueous $NaHCO_3$ solution (100 mL). The organic layer was dried, evaporated and coevaporated with toluene. The residue was purified by column chromatography with a gradient of 0 to 3% MeOH in CH_2Cl_2 containing 0.2% pyridine, to obtain 770 mg of compound **7c** (1.18 mmol, 71%) as colourless foam. ^{1}H NMR ($CDCl_3$): $\delta = 1.14$ (d, $J = 7$ Hz, 6H, CH_3), 1.93–2.41 (m, 2H, H-3′, H-3″), 2.72 (m, 1H, C*H*Me$_2$), 3.15–3.60 (m, 2H, H-5′, H-4′), 3.62–4.22 (m, 10H, H-6′, H-6″, H-1′, H-1″; s at 3.77, 2 × OCH_3), 4.79 (m, 1H, H-2′), 4.95 (d, $J = 5$ Hz, 1H, 4′-OH), 6.77 (m, 4H, aromatic H), 7.25 (m, 9H, aromatic H), 8.33 (s, 1H, H-8), 10.19 (brs, 1H, NH); ^{13}C NMR ($CDCl_3$): $\delta = 19.9$ (CH_3), 34.6 (Me$_2$*C*H), 35.2 (C-3′), 50.4 (C-2′), 55.1 (CH_3O), 60.7, 61.1 (C-4′, C-6′),

0947-6539/97/0301-0118 $ 15.00+.25/0 Chem. Eur. J. 1997, 3, No. 1

68.0 (C-1'), 82.9 (C-5'), 86.5 (Ph_3C), 139.8 (C-8), 151.0, 151.9 (C-2, C-4), 158.8 (C-6), 176.5 (C=O) and 113.0, 126.7, 127.7, 129.7, 135.6, 135.8, 144.5, 158.5 (aromatic C); LSIMS (NBA) *m/z*: 654 $[M+H]^+$; Elem. anal. ($C_{36}H_{39}N_5O_7$): calculated C: 66.14, H: 6.01, N: 10.71; found C: 66.32, H: 6.17, N: 10.47.

Synthesis of the Phosphoramidites 4a–c: A mixture of the 6'-*O*-protected nucleoside (0.5 mmol), 3 equiv of dry *N,N*-diisopropylethylamine and 1.5 equiv of 2-cyanoethyl-*N,N*-diisopropylchlorophosphoramidite in dry CH_2Cl_2 (2.5 mL) was stirred at room temperature for 3 h. After addition of EtOH (0.5 mL) and further stirring for 25 min, the mixture was washed with 5% $NaHCO_3$ solution (15 mL) and saturated NaCl solution, dried, and evaporated. Flash column chromatography afforded the amidite as a white foam, which was dissolved in a small amount of dry CH_2Cl_2 and added dropwise to cold (−50 °C) *n*-hexane (100 mL). The precipitate was isolated, washed with *n*-hexane, dried and used as such for DNA synthesis. Eluting solvent and yield after precipitation for the different amidites:

4a: *n*-hexane/ethyl acetate/Et_3N (23:75:2); 62% yield.
LSIMS (NBA) *m/z* : 759 $[M+H]^+$.

4b: *n*-hexane/ethyl acetate/Et_3N (50:48:2); 65% yield.
LSIMS (NBA) *m/z* : 872 $[M+H]^+$.

4c: *n*-hexane/acetone/Et_3N (23:75:2); 56% yield.
LSIMS (NBA) *m/z*: 854 $[M+H]^+$.

1,5-Anhydro-2,3-dideoxy-6-*O*-dimethoxytrityl-4-*O*-succinyl-2-(thymin-1-yl)-D-*arabino*-hexitol (8a): A mixture of **7a** (80 mg, 0.14 mmol), DMAP (9 mg, 0.07 mmol) and succinic anhydride (43 mg, 0.14 mmol) in anhydrous pyridine (5 mL) was stirred at room temperature for 24 h. As the reaction was incomplete an additional amount of succinic anhydride (43 mg) was added, and the mixture stirred for a further 24 h. The solution was evaporated and coevaporated with toluene. The residue was dissolved in CH_2Cl_2, the organic layer washed with saturated aqueous NaCl and water, dried and evaporated to give colourless **8a** (78 mg, 0.12 mmol, 86%).

1,5-Anhydro-2-(N^6-benzoyladenin-9-yl)-2,3-dideoxy-6-*O*-dimethoxytrityl-4-*O*-succinyl-D-*arabino*-hexitol (8b): The same procedure as described for **8a** was used for the synthesis of **8b**; **7b** (260 mg, 0.39 mmol) afforded colourless **8b** (256 mg, 0.33 mmol, 85%).

Attachment of 8a,b to Solid Supports (9a,b): A mixture of the succinates **8a,b** (80 μmol), preactivated LCAA–CPG (400 mg) [25], DMAP (5 mg, 40 μmol), Et_3N (35 μL) and 1-(3-dimethyl-aminopropyl)-3-ethylcarbodiimide·HCl (153 mg, 800 μmol) in anhydrous pyridine (4 mL) was first sonicated for 5 min and then shaken at room temperature for 16 h. After shaking, the CPG solid support was filtered off and washed successively with pyridine, methanol and CH_2Cl_2 followed by drying under vacuum. The unreacted sites on the surface of the support were capped with 1-methylimidazole (1.5 mL) in THF (Applied Biosystems) and acetic anhydride–lutidine–THF (1.5 mL, 1:1:8, Applied Biosystems). After 4 h of shaking at room temperature, the solid support was filtered off, washed with CH_2Cl_2 and dried under vacuum. Colorimetric dimethoxytrityl analysis indicated a loading of 18.5 μmol g^{-1} for **9a** and 21.5 μmol g^{-1} for **9b**.

Solid-Phase Oligonucleotide Synthesis: Oligonucleotide synthesis was performed in an ABI 381A DNA synthesiser (Applied Biosystems) by using the phosphoramidite approach. The classical synthesis protocol was used, except for the concentration of the newly synthesised products, which was increased from 0.1 to 0.13 M. The oligomers were deprotected and cleaved from the solid support by treatment with concentrated aqueous ammonia (55 °C, 16 h). After pre-purification on a NAP-10® column (Sephadex G25-DNA grade, Pharmacia) with buffer A as eluent (see below), purification was achieved on a Mono-Q® HR10/10 anion exchange column (Pharmacia) with the following gradient system [A = 10 mM NaOH, pH 12.0, 0.1 M NaCl; B = 10 mM NaOH, pH 12.0, 0.9 M NaCl; gradient used depended on the oligo; flow rate 2 mL min^{-1}]. The low pressure liquid chromatography system consisted of a Merck-Hitachi L6200 A intelligent pump, a Mono Q®-HR 10/10 column (Pharmacia), a Uvicord SII2138 UV detector (Pharmacia-LKB) and a recorder. The product-containing fraction was desalted on a NAP-10® column and lyophilised.

Melting Temperatures: Oligomers were dissolved in the following buffers: A) 1 M NaCl, 60 mM Na cacodylate, pH 7.0, 100 mM $MgCl_2$; B) 0.1 M NaCl, 10 mM Na cacodylate, pH 7.0, 10 mM $MgCl_2$; C) 0.1 M NaCl, 0.02 M potassium phosphate pH 7.5, 0.1 mM EDTA; D) 10 mM $MgCl_2$ added to buffer C; E) 1 M NaCl, 0.02 M KH_2PO_4 pH 7.5, 0.1 mM EDTA; F) 1 M NaCl, 60 mM Na cacodylate pH 7.0. The concentration was determined by measuring the absorbance at 260 nm at 80 °C and assuming the 1',5'-anhydrohexitol nucleoside analogues to have the same extinction coefficients in the denatured state as the natural nucleosides. The following extinction coefficients were used: dA and A*, $\varepsilon = 15000$; dT and T*, $\varepsilon = 8500$; dG and G*, $\varepsilon = 12500$; dC, $\varepsilon = 7500$; U, $\varepsilon = 10000$. The concentration in all experiments was ca. 4 μM for each strand unless otherwise stated. Melting curves were determined with a Uvikon 940 or with a Cary 1E (Varian, Melbourne) spectrophotometer. Cuvettes were maintained at constant temperature by means of water circulation through the cuvette holder or a thermoelectric temperature controller (Varian, Melbourne). The temperature of the solution was measured with a thermistor directly immersed in the cuvette. Temperature control and data acquisition were done automatically with an IBM-compatible computer. The samples were heated and cooled at a rate of 0.2 °C min^{-1}, and no difference could be observed between heating and cooling melting curves. Melting temperatures were evaluated by plotting the first derivative of the absorbance versus temperature curve.

CD Experiments: CD spectra were measured with a Jasco 600 spectropolarimeter in thermostatically controlled 1 cm cuvettes connected with a Lauda RCS6 Bath. The oligomers were dissolved and analysed in two different buffers: A) 1 M NaCl, 60 mM Na cacodylate, pH 7.0, 100 mM $MgCl_2$ and B) 0.1 M NaCl, 10 mM Na cacodylate, pH 7.0, 10 mM $MgCl_2$, at a concentration of 3.2 μM of each strand.

Electrophoretic Experiments: Oligonucleotides were radiolabelled (^{32}P) at the 5'-end by means of polynucleotide kinase by standard procedures [45]. To assay duplex/triplex formation, ^{32}P-labelled $(T)_{13}$ and $(dA)_{13}$ were titrated with unlabelled $(A^*)_{13}$ and $(T^*)_{13}$, respectively, and incubated for 3 min at 80 °C in 0.1 M NaCl, 0.02 M KH_2PO_4, pH 7.5, and 0.1 mM EDTA. The concentration of the ^{32}P-labelled $(T)_{13}$ and $(dA)_{13}$ was held constant throughout at 0.1 μM. The concentration of the unlabelled modified oligonucleotides varied from 0 (ratio 1:0) to 10 μM (ratio 1:100). After 1 h at room temperature, the samples were equilibrated in an ice bath for 4 h, and an equal volume of loading dye mix (40% sucrose, 0.25% bromophenol blue) was added. The samples were then loaded onto a preequilibrated (15 min at 4 °C) nondenaturing 20% polyacrylamide gel (29:1 acrylamide:*N,N'*-methylenebisacrylamide). Electrophoresis was performed at 300 V for 1 h at 4 °C (Julabo F10 cryostat) with a TB elution buffer (5 × TB: 27 g Tris base and 13.75 g boric acid in 500 mL H_2O, pH 8). The gels were visualised by autoradiography.

Enzymatic Stability: A solution of 0.4 A_{260} units of the oligonucleotides in 1 mL of the following buffer (200 mM Tris. HCl, pH 8.6, 200 mM NaCl, 28 mM $MgCl_2$) was digested with 0.04 U of snake venom phosphodiesterase (*Crotalus adamanteus* venom, Pharmacia). During digestion the increase in absorbance at 260 nm was followed. The absorption versus time curve could be fitted to an exponential curve from which the half-life could be gathered.

Acknowledgements: A. Van Aerschot is a research Associate of the Belgian Nationaal Fonds voor Wetenschappelijk Onderzoek. This work is supported by a grant from the Belgian Fonds voor Geneeskundig Wetenschappelijk Onderzoek. We are indebted to Guy Schepers for synthesis of the oligonucleotides. Many thanks to Dr. J. Rozenski for his indispensable help in computer manipulation of the CD curves.

Received: June 24, 1996 [F402]

[1] *Carbohydrate Modifications in Antisense Research, ACS Symposium Series 580* (Eds.: Y. S. Sanghvi, P. D. Cook), Washington, **1994**.
[2] F. Seela, H. Thomas, *Helv. Chim. Acta* **1995**, *78*, 94–108.
[3] F. Seela, S. Lampe, *Helv. Chim. Acta* **1994**, *77*, 1003–1017.
[4] B. C. Froehler, S. Wadwani, T. J. Terhorst, S. R. Gerrard, *Tetrahedron Lett.* **1992**, *33*, 5307–5310.
[5] K.-Y. Lin, R. J. Jones, M. Matteucci, *J. Am. Chem. Soc.* **1995**, *117*, 3873–3874.
[6] H. Rosemeyer, F. Seela, *Nucleosides, Nucleotides* **1995**, *14*, 1041–1044.
[7] R. J. Jones, K.-Y. Lin, J. F. Milligan, S. Wadwani, M. D. Matteucci, *J. Org. Chem.* **1993**, *58*, 2983–2991.
[8] Y. S. Sanghvi, P. D. Cook in *Nucleosides and Nucleotides as Antitumor and Antiviral Agents* (Eds.: C. K. Chu, D. C. Baker), Plenum, New York, **1993**, pp. 311–324.

[9] A. De Mesmaeker, A. Waldner, J. Lebretas, P. Hoffmann, V. Fritsch, R. Wolf, S. Freier, *Angew. Chem.* **1994**, *106*, 237–240; *Angew. Chem. Int. Ed. Engl.* **1994**, *33*, 226–229.
[10] S. Gryaznov, J.-K. Chen, *J. Am. Chem. Soc.* **1994**, *116*, 3143–3144.
[11] H. Inoue, Y. Hayase, A. Imura, S. Iwai, K. Miura, E. Ohtsuka, *Nucl. Acids Res.* **1987**, *15*, 6131–6148.
[12] a) M. Perbost, M. Lucas, C. Chavis, A. Pompon, H. Baumgartner, B. Rayner, H. Griengl, J.-L. Imbach, *Biochem. Biophys. Res. Commun.* **1989**, *165*, 742–747; b) H. E. Moser in *Perspectives in Medicinal Chemistry* (Eds.: B. Testa, E. Kiburz, W. Fuhrer, R. Giger), VHCA & VCA, Basel, **1993**, pp. 275–297.
[13] C. Gagnor, J.-R. Bertrand, S. Thenet, M. Lemaître, F. Morvan, B. Rayner, C. Malvy, B. Lebleu, J.-L. Imbach, C. Paoletti, *Nucl. Acids Res.* **1987**, *15*, 10419.
[14] R. S. Varma, *Synlett* **1993**, 621–637.
[15] H. Wang, D. D. Weller, *Tetrahedron Lett.* **1991**, *32*, 7385–7388.
[16] B. Hyrup, P. E. Nielsen, *Bioorg. Med. Chem.* **1996**, *4*, 5–23.
[17] S. L. Beaucage, R. P. Iyer, *Tetrahedron* **1993**, *49*, 6123–6194.
[18] A. Eschenmoser, *Pure Appl. Chem.* **1993**, *65*, 1179–1188.
[19] A. Eschenmoser, M. Dobler, *Helv. Chim. Acta* **1992**, *75*, 218–259.
[20] J. Hunziker, H.-J. Roth, M. Böhringer, A. Giger, U. Diederichsen, M. Göbel, R. Krishnan, B. Jaun, C. Leumann, A. Eschenmoser, *Helv. Chim. Acta* **1993**, *76*, 259–352.
[21] K. Augustyns, A. Van Aerschot, C. Urbanke, P. Herdewijn, *Bull. Soc. Chim. Belg.* **1992**, *101*, 119–130.
[22] A. Augustyns, F. Vandendriessche, A. Van Aerschot, R. Busson, C. Urbanke, P. Herdewijn, *Nucl. Acids Res.* **1992**, *20*, 4711–4716.
[23] A. Augustyns, G. Godard, C. Hendrix, A. Van Aerschot, J. Rozenski, T. Saison-Behmoaras, P. Herdewijn, *Nucl. Acids Res.* **1993**, *21*, 4670 4676.
[24] P. Herdewijn, H. De Winter, B. Doboszewski, I. Verheggen, K. Augustyns, C. Hendrix, T. Saison-Behmoaras, C. De Ranter, A. Van Aerschot in *Carbohydrate Modifications in Antisense Research, ACS Symposium Series 580* (Eds.: Y. S. Sanghvi, P. D. Cook), Washington, **1994**, Chapt. 6.
[25] I. Verheggen, A. Van Aerschot, L. Van Meervelt, J. Rozenski, L. Wiebe, R. Snoeck, G. Andrei, J. Balzarini, P. Claes, E. De Clercq, P. Herdewijn, *J. Med. Chem.* **1995**, *38*, 826–835.
[26] C. Pannecouque, F. Vandendriessche, J. Rozenski, G. Janssen, R. Busson, A. Van Aerschot, P. Claes, P. Herdewijn, *Tetrahedron* **1994**, *50*, 7231–7246.
[27] I. Verheggen, A. Van Aerschot, S. Toppet, R. Snoeck, G. Janssen, J. Balzarini, E. De Clercq, P. Herdewijn, *J. Med. Chem.* **1993**, *36*, 2033–2040.
[28] G. Ti, B. Gaffney, R. Jones, *J. Am. Chem. Soc.* **1982**, *104*, 1316–1319.
[29] *Oligonucleotides: A Practical Approach* (Ed. M. Gait), IRL, Oxford, **1984**.
[30] R. Pon, N. Usman, K. Ogilvie, *Biotechniques* **1988**, *6*, 768–775.
[31] D. Riesner, R. Romer, *Physicochemical Properties of Nucleic Acids, Vol. II.* (Ed.: J. Duchesne), Academic Press, London, **1973**, 237–318.
[32] M. J. D. Powell, *Comp. J.* **1965**, *7*, 303–307.
[33] U. Neidlein, C. Leumann, *Tetrahedron Lett.* **1992**, *33*, 8057–8060.
[34] D. S. Pilch, C. Levenson, R. H. Shafer, *Biochemistry* **1991**, *30*, 6081–6087.
[35] S. M. Gryaznov, D. H. Lloyd, J.-K. Chen, R. G. Schultz, L. A. DeDionisio, L. Ratmeyer, W. D. Wilson, *Proc. Natl. Acad. Sci.* **1995**, *92*, 5798–5802.
[36] H. Rosemeyer, M. Krecmerova, F. Seela, *Helv. Chim. Acta* **1991**, *74*, 2054–2067.
[37] D. S. Pilch, C. Levenson, R. H. Shafer, *Proc. Natl. Acad. Sci.* **1990**, *87*, 1942–1946.
[38] H. Rosemeyer, F. Seela, *Helv. Chim. Acta* **1991**, *74*, 748–761.
[39] a) G. S. Manning, *Q. Rev. Biophys.* **1978**, *11*, 179–246; b) M. T. Record, Jr., C. F. Anderson, T. M. Lohman, *ibid.* **1978**, *11*, 103–178.
[40] A. Van Aerschot, I. Verheggen, C. Hendrix, P. Herdewijn, *Angew. Chem.* **1995**, *107*, 1483–1485; *Angew. Chem. Int. Ed. Engl.* **1995**, *34*, 1338–1339.
[41] E. Henderson, C. C. Hardin, S. K. Walk, I. Tinoco, Jr., E. Blackburn, *Cell* **1987**, *51*, 899–908.
[42] A. Van Aerschot, T. Saison-Behmoaras, J. Rozenski, C. Hendrix, G. Schepers, G. Verhoeven, P. Herdewijn, *Bull. Soc. Chim. Belg.* **1995**, *104*, 717–720.
[43] F. Seela, K. Kaiser, *Nucl. Acids Res.* **1987** *15*, 3113–3129.
[44] M. Cooney, G. Czernuszewicz, E. H. Postel, S. J. Flint, M. E. Hogan, *Science* **1988**, *241*, 456–459.
[45] T. Maniatis, E. Fritsch, J. Sambrook, *Molecular Cloning: A Laboratory Manual* (Cold Spring Harbor Laboratory, New York), **1989**.
[46] J.-P. Shaw, K. Kent, J. Bird, J. Fishback, B. Froehler, *Nucl. Acids Res.* **1991**, *19*, 747–750.

0947-6539/97/0301-0120 $ 15.00+.25/0